MEASUREMENT OF WATER TEMPERATURE AND VELOCITY FIELDS BY APPLYING THERMOGRAPHY ON TWO-PHASE FLOW THROUGH HORIZONTAL RECTANGULAR CHANNEL

by

Darius LAURINAVICIUS [*]***, Marijus SEPORAITIS, Mindaugas VALINCIUS, and Stasys GASIUNAS***

Lithuanian Energy Institute, Kaunas, Lithuania

Original scientific paper
https://doi.org/10.2298/TSCI160502129L

The infrared thermography and optical-flow based method were proposed for the measurement of water temperature and velocity fields in stratified steam-water flow through horizontal channel. Generally, this method is applicable for any turbulent flow with temperature gradient. Spinel polycrystalline ($MgAl_2O_4$) material was chosen for infrared optical window, as, besides excellent optical properties, it has exceptional durability in harsh environment. Different mounting types and dimensions were tested in order to investigate Spinel application possibilities and limitations. A significant influence of window specific thermal radiation on measurement results (>20% inaccuracy) was observed during experiments. The best identified configuration ensures good temperature measurement accuracy (<=2%). Graphical analysis was applied to infrared images, and good results of turbulence structure identification were achieved using combined local-global optical flow technique.

Key words: *infrared camera, thermocouple, two-phase flow, rectangular channel, temperature, optical flow*

Introduction

In last two centuries, flow temperature and velocity were measured by thermometers, thermocouples, thermal resistors, Pitot tubes, hotwire anemometers, *etc*. [1]. All these measurement devices were used in various industries, civil, mechanical engineering infrastructure, science, aerospace objects, and power plants. In general, this equipment is contact type and does not provide a visual image of the flow under investigation [2]. Also, in particular cases, like investigation of gaseous or liquid materials, these devices directly disturb the flow. Therefore, in different industries, devices for measuring temperature, velocity, and pressure without physical contact have recently become widely used [3], and this is known as non-intrusive control. One of non-intrusive methods is thermography. It allows measuring temperature or heat flux using infrared camera. This method is applied in different facilities like power plants, chemical factories, civil buildings, science, *etc*.

In science, thermography is also quite a new method. It allows observing different phenomena in more detail with high resolution, which is especially useful for investigation of unsteady two-phase flow [4], and it can provide direct observation of thermal hydraulic features related to boiling [5]. The thermography method can be applied in different investigations of

[*] Corresponding author, e-mail: darius.laurinavicius@lei.lt

one or two-phase flows. Nelson developed the characterization and visualization of liquid spray technique. It uses an infrared thermography based measurement, in which a uniformly heated background acts as a thermal radiation source, and an infrared camera as the receiver [6]. The unsteady heating and acoustic streaming, generated by a high intensity acoustic horn in a thermo-viscous fluid, were investigated by Christopher *et al.* [7]. They have measured surface heating profiles using infrared camera. Golobic *et al.* [8] have investigated bubble growth and coalescence during boiling of water on a titanium foil. Wall temperature measurements on the back of the foil by high speed infrared camera, synchronized with high speed video camera recording bubble motion, were carried out. Karthikeyan *et al*. [4] have focused on understanding of the pulsating heat pipe operation with spatial and temporal measurement of temperature by high-resolution infrared thermography. Volino and Smith [9] have presented simultaneous measurements of surface temperature and the underlying velocity field for thick horizontal layer evaporatively cooled from above. The authors used an infrared sensing array to capture the instantaneous free surface temperature field. Mehta and Khandekar [10] experimentally determined the local heat transfer coefficient along stream-wise direction in single-phase internal convective flows. Their study focused on the very early part of the development of the thermal boundary-layer, wherein the transport coefficients, as well as their axial gradient, along the stream-wise directions are very high, and the measurement was challenging. Haber *et al*. [11] have measured the temperature profiles of the fast and exothermic hydrolysis inside micro capillaries via infrared transparent window. The heat transfer coefficient of micro reactor cooling system was determined by thermal imaging. Mehta and Khandekar [12] have presented an experimental design method so that local heat transfer could be estimated by minimizing the conjugate heat transfer effects in the system by employing high-resolution infrared camera. Charogiannis *et al*. [13]presented experimental technique based on method of thermography, which was capable of the simultaneous measurement of 2-D surface temperature and velocity at the surface of multiphase flow. From recent publications, it is seen that thermography method is quite broadly applied for investigation in one or two-phase flows. But in particular cases, the thermography method is restricted by several limitations, like body surface emissivity, the correct geometrical identification of measured points, and the design of the optical access window, including the choice of the most appropriate infrared material [14].

The aim of this study was to employ the thermography method for measuring water temperature field dynamics and evaluating turbulence in a horizontal stratified two-phase flow. Measurement of water temperature was heavily influenced by the vicinity of cold and hot fluids. Therefore, water temperature measurement error exceeded 20%. Major part of this error comes from thermal emission of optical window material. The method of water temperature measurement for stratified two-phase flow with ~75 K difference of steam and water bulk temperatures is presented. Water turbulence structure was determined by applying hybrid Lucas-Kanade and Horn-Schunck optical flow (OF) evaluation method [15] on infrared images sequence.

Infrared measurement method

Objects with temperature higher than –273.15 °C (0 K) emit electromagnetic radiation in infrared range [1]. Infrared range is divided into: near infrared (0.75-3.00 μm), middle infrared (3-6 μm), far infrared (6-15 μm), and extreme infrared (15-1000 μm) [16]. Infrared imaging equipment operates in two different bands: short wave (3-6 μm) and long wave (8-12 μm). In this work, FLIR SC5000 was used, which operates in 2.5-5.1 μm band.

Infrared camera receives radiation from the object and radiation from surrounding environment, which is reflected from the object, fig. 1. This radiation is partly absorbed by the atmosphere. From here, the third radiation source comes from the atmosphere.

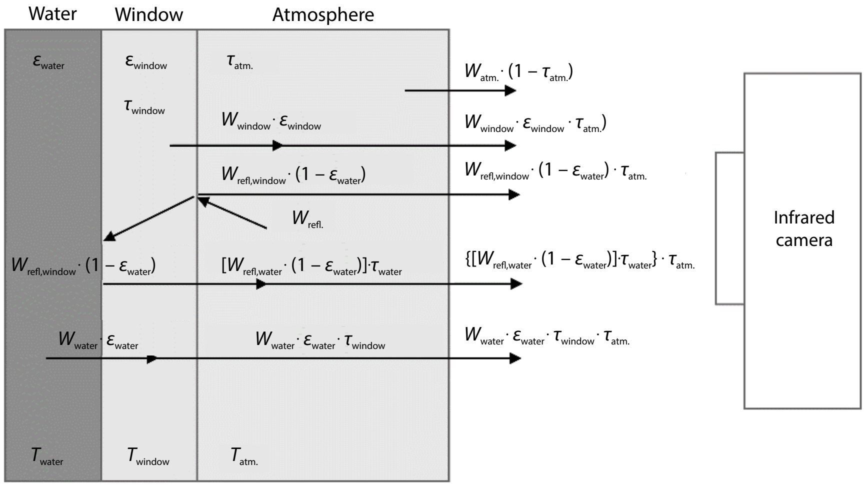

Figure 1. A schematic representation of the general thermographic measurement set-up

The total radiation power, W_{tot}, which is collected by infrared camera, can be described:

$$W_{\text{tot.}} = \overbrace{W_{\text{window}}\varepsilon_{\text{window}}\tau_{\text{atm.}}}^{1} + \overbrace{W_{\text{refl.,window}}\left(1-\varepsilon_{\text{water}}\right)\tau_{\text{atm.}}}^{2} + \overbrace{W_{\text{atm.}}\left(1-\tau_{\text{atm.}}\right)}^{3} + \\ + \overbrace{W_{\text{refl.,water}}\left(1-\varepsilon_{\text{water}}\right)\tau_{\text{window}}\tau_{\text{atm.}}}^{4} + \overbrace{W_{\text{water}}\varepsilon_{\text{water}}\tau_{\text{window}}\tau_{\text{atm.}}}^{5} \quad (1)$$

The 1st component is emission from the window, where $\varepsilon_{\text{window}}$ is the emittance of window, and is transmittance of the atmosphere. The object temperature is T_{wind}. The 2nd – reflected emission from ambient sources, where $(1 - \varepsilon_{\text{water}})$ is the reflectance of the window. The 3rd – emission from the atmosphere, where $(1 - \tau_{\text{atm}})$ is the emittance of the atmosphere. The 4th member is the same like 2nd, it just is refractived from interface of window/water $(1 - \varepsilon_{\text{water}})$. The τ_{window} and transmitted through window and atmosphere. The 5th component is emission from the water, where $\varepsilon_{\text{water}}$ is the emittance of water, and τ_{window} is transmittance of the window. All five components are important in processing the measurements of temperature.

Therefore, the operator must correctly enter values of these parameters:
– emittance coefficients $(\varepsilon_{\text{water}})$ and $(\varepsilon_{\text{window}})$ of the water and window,
– distance between object and camera, $D_{\text{obj.}}$,
– the temperature of surrounding objects or reflected ambient temperature, T_{refl}, and
– the temperature of atmosphere and window, T_{atm} and T_{window}.

The measurement of low temperatures is more critical than of high temperatures, *i. e.*, the measurement error will be smaller when the temperature of the object is higher.

When the temperature of the object is similar to the environment, the error of measurement is larger due to relative larger radiation *disturbances* from other sources. Consequently, processing of the object temperature measurements is necessary for removing or isolating other infrared sources.

The primary idea of the experimental design was to develop and implement a non-intrusive method for measuring water temperature profiles in stratified two-phase (steam/water) flow in a horizontal channel. The thermography method was chosen, because it allows measuring temperature with high resolution (~25 points/mm^2) and allows thermal tracking of water turbulence with its analysis later. All temperature data can be recorded at 25-175 frames per second.

However, thermography method can measure water temperature only near optical window wall (20-30 μm depth) due to high water emission coefficient.

The test channel is made of stainless steel with inner dimensions of 1000 × 100 × 20. Spinel ($MgAl_2O_4$) metal ceramics optical window is mounted in sidewall.

An adequate installation method, which mitigates errors coming from window own radiation, has been found during designing and testing the experimental setup for measurement of temperature distribution using infrared camera.

At first, the analysis of available infrared materials and decision on the choice one for the optical window has to be performed. The majority of infrared transmitting materials are within the range of 3-5 μm, and only several are in 8-14 μm. [17]. All these materials have different properties (transmittance, emittance, thermal shock resistance, thermal conductivity coefficient), which were evaluated separately for water temperature measurement in stratified two-phase flow.

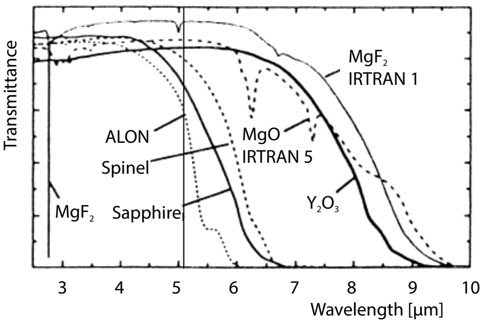

Figure 2. Infrared transmittance coefficients of various infrared grade optical materials [17]

Transmittance is the fraction of incident electromagnetic radiation at a specified wavelength that passes through a window. These materials $MgAl_2O_4$, MgF_2, MgO, Al_2O_3, Y_2O_3 have the best transmittance in 2.5-5.1 μm band, fig. 2.

Emittance (emission) is very important when measuring high temperature of liquid or gaseous materials. Emission coefficient shows what part of energy the material radiates as compared to a black body. The infrared emission spectrum of the material depends on its temperature. When the temperature of the material increases, the emission also increases. This window property becomes critical when water temperature is measured near steam/water interface. If two different temperature fluids have a direct contact with the optical window, the heat from the hotter (due to conductivity effect) fluid through optical windows flows to the colder fluid, fig. 3.

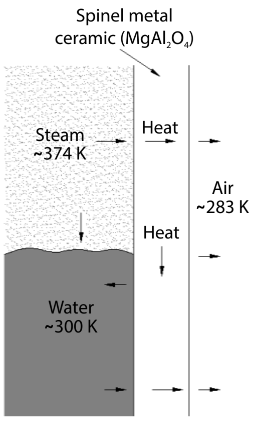

Figure 3. Principle scheme of heat transportation

Therefore, the material of the optical window becomes warmer than the cold fluid behind it. As a result, the infrared camera will receive additional optical window material radiation. The following conditions create an uncertainty in water temperature measurements.

In fig. 4(a), emission coefficient of different window materials is compared at the window temperature 700 K [17]. Yttria has the smallest coefficient of emission, which varies from 0 to 0.01. Spinel has the second smallest emission, which varies from 0 to 0.25 (3.05.1 μm range). Figure 4(b) shows emission distribution of 2 mm thick Spinel window at different temperatures. At 373 K, the emission is ~0.13 within 3.0-5.1 μm band. In order to increase the accuracy of water temperature measurement, the infrared filter may be used to cut off the undesirable window infrared

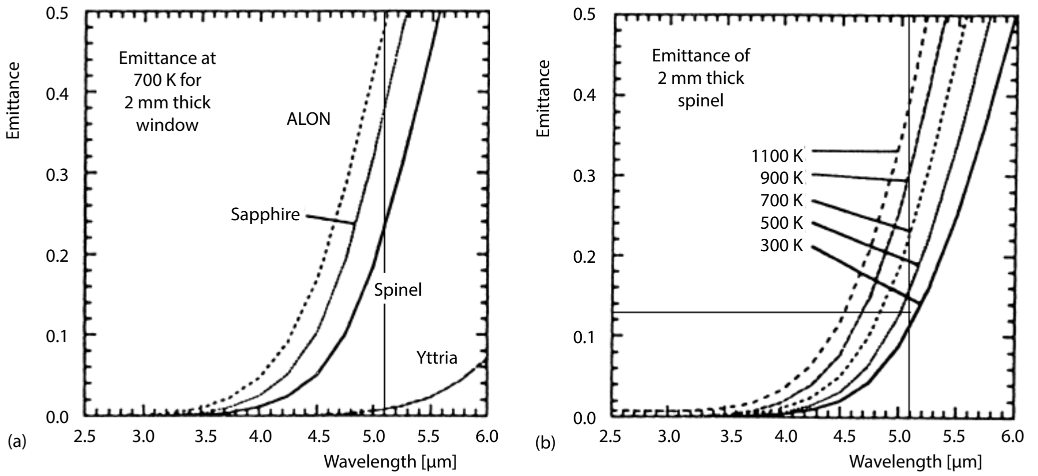

Figure 4. Emittance of optical window materials (computed) [17]; (a) comparison of ALON, sapphire, spinel and yttria at 700 K, (b) emittance coefficient of spinel at different temperatures

emissivity part. For Spinel wavelength over 4.0 µm should be cut. But substantial amount of all radiation would be lost, too. In case of high grade infrared filters – about 20%. Additionally, on infrared camera images, an undesirable interference pattern (Newton's rings) will be created by the reflection of between camera lenses and filter.

Thermal shock resistance is very important when two stratified fluids with a large temperature difference (~80K) contact with the window. Large temperature gradient at steam water interface can cause optical window cracking. Metal ceramic – Spinel material has good thermal shock resistance related characteristics; therefore, it is used for infrared transparent domes of military missiles [18]. In future, the promising infrared inert and transparent material are Yttrium oxide or Yttria/Magnesia composites, which still are under development [19, 20] and not available in stock.

Table 1. Properties of infrared materials [18]

Material	Flexural strength [MPa]	Young's modulus [GPa]	Poisson's ratio	Thermal conductivity [$Wm^{-1}K^{-1}$]	Thermal exp. coefficient [$10^{-6}K^{-1}$]
Al_2O_3	500	400	0.27	24	7
ALON	300	317	0.24	13	7
Diamond	2000	1050	0.16	2000	1
GaAs	60	86	0.31	53	6
GaP	100	103	0.31	97	6
MgF_2	100	115	0.30	12	10
$MgAl_2O_4$	180	280	0.26	15	8
Y_2O_3	150	170	0.30	14	7
ZnS	100	74	0.29	17	7
ZnSe	50	71	0.21	13	8

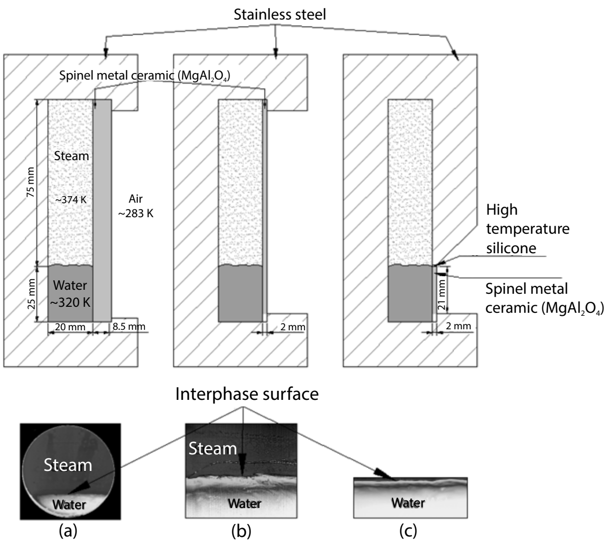

Figure 5. Three installation mods (A, B, C) of Spinel optical windows and resulting IR images

So, after evaluation of all these parameters, Spinel was chosen as the optimal material. It has one of the largest transmittance coefficients (0.85) in the range 2.55.1 μm and one of the lowest emittance coefficients (0.14) at ~374 K (101°C). Also spinel has good resistance to thermal shock, and its thermal conductivity is quite low (15 W/mK), tab. 1.

Three different installation cases of spinel optical window were examined, fig. 5, and the results were compared. The examination of three windows was made for stratified two-phase flow flowing in the rectangular channel, when water velocity was 0.056 m/s, steam velocity –6 m/s, water inlet temperature –298 K (25°C).

The experimental study was carried out in the following sequence:

– setting of inlet water (0.014 m/s) and steam (6 m/s) velocities, temperature, 298 K (25°C), and height (25 mm) of water level,
– letting the entire system achieve steady-state (channel temperatures becomes constant after ~3 hours), and
– water temperature using infrared camera and thermocouple was measured for 30 seconds simultaneously at the same position in the channel. Temperature profiles were acquired by infrared camera at 50 fps (1500 thermal images) and thermocouple at 1 Hz (30 readings); the infrared camera and thermocouple data values were averaged separately; the results are demonstrated in fig. 8.

Infrared-optical flow method for turbulence structure analysis

Generally, water velocity fields can be accurately measured by using laser doppler anemometry (LDA) and particle image velocimetry (PIV) techniques. The LDA method is the most precise, but it is only a single-point measurement technique. Therefore, it is unsuitable for the measurement of large unsteady vortices. Another LDA disadvantage is that sequential measurements by probe traversing have to be made in order to acquire velocity profile or the entire field. The PIV-based flow measurement alleviates most of these concerns. The PIV allows measuring the entire 2-D field at once, and even full three component 3-D measurement is feasible thorough the adjustable-depth volume PIV techniques. In terms of velocity data obtaining principle, the alternative infrared-OF method, proposed in this work, is somewhat similar to PIV, as it also uses recorded video data frames for 2-D water velocity field analysis. The infrared-OF method relies on the fact that sequence of infrared images contains information not only about temperature field dynamics, but also about the water motion. The movement of different temperature eddies in non-laminar flow allows the visual perception of turbulence. Mathematical processing of thermal field data is needed for the objective flow structure assessment. As the goal is the evaluation of motion, the vector fields have to be calculated by analysing differences between the infrared frame pairs. It can be done by direct comparison of temperature value matrices, but a more rational approach is the utilisation of well-developed algorithms from the graphical analysis. The OF technique was developed for detecting motion of large objects at a real world scene, but, properly applied to the infrared images of flow, it appears to be an interesting alternative offering high evaluation accuracy. For OF analysis instead of temperature value in each point, the temperature representing brightness level is used as data input. Of course, because the data are taken from infrared images, the resulting patterns of water motion are determined only in the vicinity of the optical window.

Typical OF technique consists of 3 main stages [15]:

- primary filtering or smoothing using *low pass*/*band pass* filter in order to extract the signal of interest structure and to enhance signal-to-noise ratio,
- basic data extraction, such as the derivatives of time and space (evaluation of components of normal velocity) or local correlation surface, and
- the integration of these data in order to get the 2-D flow field, which is often based on assumptions about the smoothness of the underlying flow field.

Different OF methods are classified in [21]:

- *differential* techniques compute velocity from spatio-temporal derivative of image intensity or filtered versions of the image (using low pass or band-pass filters),
- *region-based matching* method is based on the best match amounts to maximize a similarity measure, such as the normalized cross-correlation or minimizing a distance measure, such as the sum-of-squared difference,
- *energy-based* methods are based on the output energy of velocity-tuned filters; these are also called frequency-based methods owing to the design of velocity-tuned filters in the Fourier domain, and
- *phase-based* techniques; here velocity is defined in terms of the phase behaviour of band-pass filter outputs.

Several OF analysis methods were tried by changing of their parameters, but an adequate sensitivity for water turbulence has not been reached. Wilde *et al*. [15] presented the combined local-global (CLG) approach by Bruhn *et al*. [22] which encompasses properties of HS (Horn and Schunk [23]) and LK (Lucas and Kanade [24]), aiming to improve the OF accuracy for small-scale variations, while delivering the dense and smooth fields. Consequently, this method is the most suitable for detecting turbulence of water flow using infrared images. The main parameters for CLG calculation and optimal settings used in infrared-OF:

- Global smoothing coefficient $\alpha > 0$ (higher values of α yield more homogeneous fields, while lower values allow more dissimilar displacement vectors) $\alpha = 20$.
- Local spatio-temporal derivative smoothing term defined as a convolution between a 2-D Gaussian kernel with standard deviation ρ (when $\rho = 0$, no local smoothing occurs.) $\rho = 50$.
- Gaussian image smoothing parameter $\sigma = 0$ (default setting).
- Successive over-Relaxation (SOR) coefficient $0 < w < 2$, $w = 1.8$.
- The number of scales, provided that the final size of the coarsest pyramid level is large enough to compute the derivatives *n_scales* = 10 (if not defined, the maximum scale number is computed and used).
- Pyramid-resizing factor 0 < scale_Factor < 1 *scale_Factor* = 0.5 (default setting).
- The iteration mode SOR or Pointwise-Coupled Gauss-Seidel *coupledMode* = 0 (more accurate SOR).

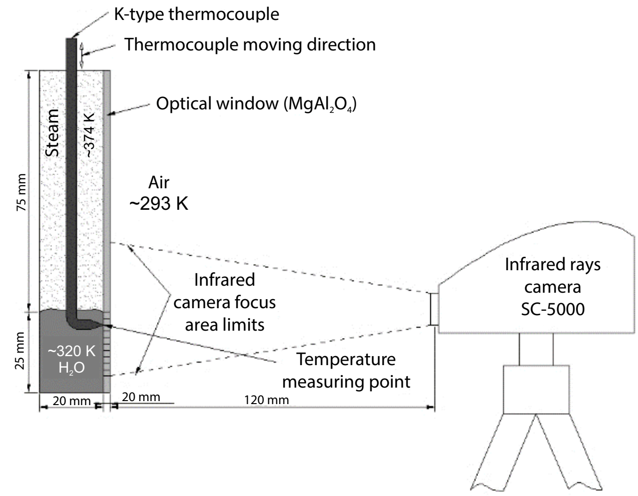

Figure 6. Water and steam temperature measuring scheme using infrared camera and thermocouple

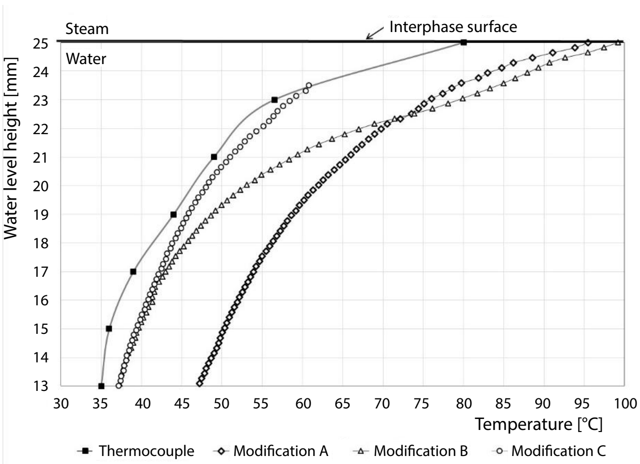

Figure 7. Measurements of water temperature profiles through circle (8.5 mm thick, 90 mm diameter, *A mod.*), rectangular (100 × 90 × 2 mm, *B mod.*), rectangular optical windows (100 × 25 × 2 mm, *C mod.*) using infrared camera and thermocouple

Infrared measurement results

A mod. The first Spinel optical window was round, flat, 8.5 mm thick, fig. 6(a). It was installed in the sidewall of a rectangular channel. The water temperature was simultaneously measured at the same locations using infrared camera and thermocouple, fig. 6.

Results of water temperature measurement by infrared camera had much higher values, fig. 7, *A mod*. Temperature overestimation was ~1520 K near water/steam interphase, above 21 mm of water level. Going deeper, the infrared overestimation decreases. Such overestimation of water temperature by using infrared method is mainly the result of Spinel conductivity. The conjunction of window conductivity and emissivity parameters with larger thickness of 8.5 mm leads to substantial amount of heat transferring from steam to water through optical window and additional infrared radiation from the window material itself.

Steam temperature was measured correctly by infrared camera and thermocouple. Uncertainty of thermocouples ±1 K, infrared camera - ±1 K or ±1%. Within near interphase area (23-25 mm), the temperature difference was ~ 15-20 K. The largest difference (~17-20 K) was at the 17-23 mm water level. From 17 mm to 13 mm, the temperature measurement difference between infrared and thermocouple decreased to ~9-10 K.

B mod. The second tested window was rectangular, flat, 2.0 mm thick, (fig. 5. *B mod.*) The window installation and test procedure were similar to those of *A mod*., fig. 7. In this case, the largest overestimation of water temperature was about ~17-20 K at interface, fig. 7, *B mod.* , and 25 mm. But comparison of *A* and *B mods* shows a substantial increase in accuracy of water temperature measurement. At the water level of 22 mm and under it, the temperature overestimation was less than 3-4 K.

C mod. In this test, the optical infrared window was installed only within the water area, fig. 5, *C mod.* , in order to minimize its contact with steam. For sealing the window to the stainless steel wall, silicone rubber sealant was used. The thermal conductivity coefficient of silicone (1.3 W/mK) is very low compared with steel (22 W/mK) or Spinel (14 W/mK). So, silicone reduces window heat up from the steel wall, which is heated by steam. In that case, the water temperature overestimation does not exceed 2 K (fig. 7, *C mod.*). If the amplitude of water waves is high, the upper edge of the window still can be exposed to steam in periodic manner and slightly heat up. In other cases, when interphase is smooth, the temperature measured by infrared camera differs only by ~2 K from that measured by thermocouple.

The detection of water/steam level using thermocouple probe is quite problematic due the refraction index of optical window. Therefore, thermocouple is positioned a little lower (~0.5 mm) than the actual interphase, and upper point temperature measured by thermocouple is much lower than 373 K. That is due to a very steep temperature gradient near the interphase area.

Infrared-OF analysis of flow turbulence

The 2-D vector fields of water turbulence in horizontal stratified cocurrent two-phase flow are provided in figs. 8 and 9. If steam velocity is higher than water velocity, the interfacial

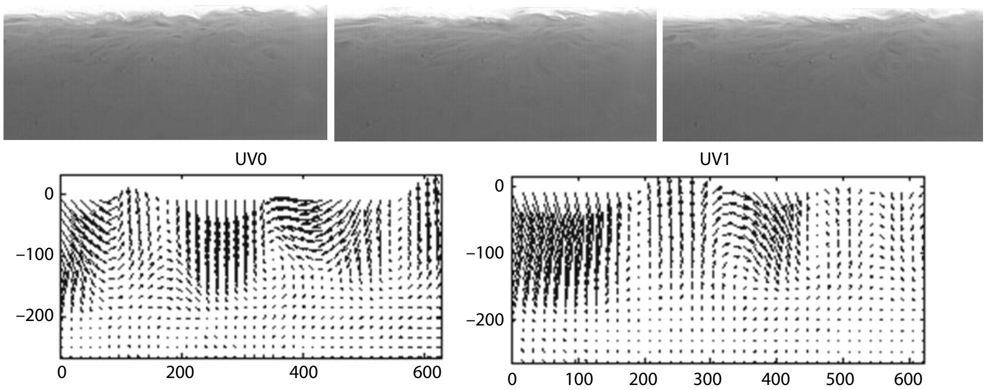

Figure 8. Sequence of infrared images and OF calculated vector fields near interfacial turbulence in water

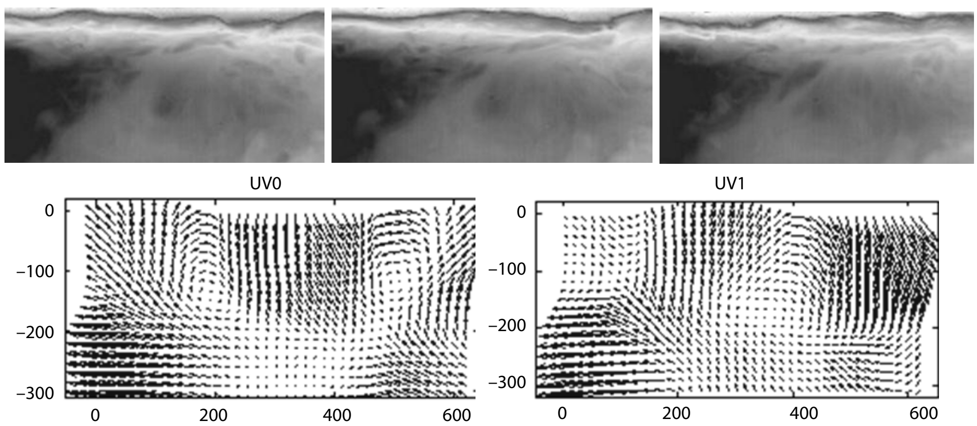

Figure 9. Sequence of infrared images and OF calculated vector fields turbulence outspread in all water layer

shear generates turbulence in water. The OF algorithm treats moving zones with distinctive temperature as objects. With the aforementioned (in the previous chapter) parameters, it is tuned to track turbulence, but ignores bulk flow by being much more sensitive to transverse movement of water gusts (length much greater than width).

The average velocity of water was 0.055 m/s, and infrared camera frame rate – 50 Hz. So, in case of the uniform flow, the displacement between two frames would be only 1 mm. However, because of high two-phase slip ratio (over 100), water velocity near interface was about 10 times higher than the average. Therefore, at least 200 Hz is needed for accurate tracking of vortices in flow with local velocity of ~0.5 m/s. The treatment of the temperature matrix as optical image allows usage of initial filtering, smoothing or other photo filters to extract the signal of interest and increase the signal to noise ratio. Thus, CLG OF approach can be successfully applied for digital processing of infrared images to calculate and visualize flow turbulence.

Concluding remarks and recommendations

A thermography method and OF technique were successfully applied to measure water temperature profiles and visualise of condensing two-phase flow structure. Different infrared transparent materials and influence of their properties on optical window performance were evaluated. The study showed that Spinel metal ceramic is the optimal material for the optical window. It has high transmittance (0.85), low emittance (max. 0.14, at window temperature ~400 K), and good resistance to thermal shock (exp. coeff. 8.1E-6 1/K).

Three different (A, B, and C) window installations were examined, and their influence on accuracy of water temperature measurements was tested. The infrared camera measurement was compared to thermocouple.

Testing showed that thick spinel window (8.5 mm *A mod*.) gives overestimation of ~17-20 K. However, thick optical window only adds additional infrared radiation as positive error. Its transmittance is good enough for qualitative estimation of dynamics in temperature field and thermal flows. So, thermography through 8.5 mm spinel still can be considered as rational for high pressure systems (vessels, pipes).

Thinner spinel window (2.0 mm *B mod*.) shows much better results – such large overestimation occurs only near steam/water interface. This should be taken into account if measurement is made through optical window which have direct contact not only with water, but also with hot steam.

The same as in *B mod*. thickness, but installed only in water area spinel (*C mod*.) showed best temperature measurement accuracy (~2 K overestimation).

In general, the method of infrared thermography through optical window showed up as descent alternative to more complicated methods (if its limitations are acceptable). The thinner windows and minimised contact to steam is recommended for the best results. In order to achieve the highest accuracy, the additional cut-off filter for 2.5-4.0 μm may be used or Y_2O_3 material instead of spinel should be chosen for the optical window.

Combined global-local optical flow technique was successfully applied for digital processing of infrared images to calculate and visualize flow turbulence structure. If the quantitative parameter is needed, it can be deduced from resulting OF vector fields by additional statistical post processing.

References

[1] Wang, W., *et al.*, Analysis of Infrared Temperature Measurement for Flue Gas Shielding Metal Surface Using Source Multi-Flux Method, *Thermal Science*, *22* (2016), 1, pp. 313-321

[2] Bagavathiappan, S., *et al*., Infrared Thermography for Condition Monitoring – A Review, *Infrared Physics and Technology*, *60* (2013), Sept., pp. 35-55
[3] Tartarini, P., *et al*., Dropwise Cooling: Experimental Tests by Infrared Thermography and Numerical Simulations, *Applied Thermal Engineering, 29* (2009), 7, pp. 1391-1397
[4] Karthikeyan, V. K., *et al*., Infrared Thermography of a Pulsating Heat Pipe: Flow Regimes and Multiply Steady States, *Applied Thermal Engineering*, *62* (2014), 2, pp. 470-480
[5] Yoo, J., *et al*., An Accurate Wall Temperature Measurement Using Infrared Thermometry with Enhanced Two-Phase Flow Visualization in a Convective Boiling System, *International Journal of Thermal Sciences*, *90* (2015), Apr., pp. 248-266
[6] Nelson, K. A., *et al*., Infrared Thermography-Based Visualization of Droplet Transport in Liquid Sprays, *Infrared Physics and Technology*, *53* (2010), 3, pp. 218-226
[7] Christopher, N., *et al*., Characterization of Acoustic Streaming and Heating Using Synchronized Infrared Thermography and Particle Image Velocimetry, *Ultrasonic Sonochemistry*, *18* (2011), 5, pp. 1258-1261
[8] Golobic, I., *et al*., Bubble Growth and Horizontal Coalescence in Saturated Pool Boiling on a Titanium Foil, Investigated by High-Speed IR Thermography, *International Journal of Heat and Mass Transfer, 55* (2012), 4, pp. 1385-1402
[9] Volino, R. J., Smith, G. B., Use of Simultaneous IR Temperature Measurements and DPIV to Investigate Thermal Plumes in a Thick Layer Cooled from above, *Experiments in Fluids*, *27* (1999), 1, pp. 70-78
[10] Mehta, B., Khandekar, S., Infrared Thermography of Laminar Heat Transfer during Early Thermal Development Inside a Square Mini-Channel, *Experimental Thermal and Fluid Science, 42* (2012), Oct., pp. 219-229
[11] Haber, J., *et al*., Infrared Imaging of Temperature Profiles in Microreactors for Fast and Exothermic Reactions, *Chemical Engineering Journal, 214* (2013), Jan., pp. 97-105
[12] Mehta, B., Khandekar, S., Measurement of Local Heat Transfer Coefficient during Gas-Liquid Taylor Bubble Train Flow by Infra-Red Thermography, *International Journal of Heat and Fluid Flow, 45* (2014), Feb., pp. 41-52
[13] Charogiannis, A., *at al*., Thermographic Particle Velocimetry (TPV) for Simultaneous Interfacial Temperature and Velocity Measurements, *International Journal of Heat and Mass Transfer, 97* (2016) June, pp. 589-595
[14] Hetsroni, G. *et al*. Infrared Temperature Measurements in Micro-Channels and Micro Fluid Systems, *International Journal of Thermal Sciences*, *50* (2011), 6, pp. 853-868
[15] Wilde, J. J., *at al*., An Implementation of Combine Local-Global Optical Flow, *Image Processing on Line, 5* (2015), June, pp. 139-158
[16] Carosena, M., Giovanni, M. C., Recent Advances in the Use of Infrared Thermography: Review Article, *Measurements Science and Technology, 150* (2004), 9, pp. R27-R58
[17] Harris, D. C., Durable 3-5 μm Transmitting Infrared Window Materials, *Infrared Physics & Technology*, *39* (1998), 4, pp. 185-201
[18] Klein, C. A., Infrared Missile Domes: Heat Flux and Thermal Shock, *High Heat Flux Engineering II, 1997* (1993), Nov., pp. 150-169
[19] Kong, L. B., *et al*., *Transparent Ceramics*, Springer International Publishing XII, New York, USA, 2015, p. 734
[20] Wang, J., *et al*., Densification of Yttria Transparent Ceramics: The Utilization of Activated Sintering. *Journal of the American Ceramic Society*, *99* (2016), 5, pp. 1671-1675
[21] Barron, J. L., *et al*., Performance of Optical Flow Techniques, *International Journal of Computer Vision*, *12* (1994), 1, pp. 43-77
[22] Bruhn, A., *et al*., Combining the Advantages of Local and Global Optic Flow Methods, in: *Pattern Recognition*, (Ed. Luc Van Gool), Vol. 2449 of Lecture Notes in Computer Science, Spinger Berlin, Heidelberg, 2002, pp. 454-462
[23] Horn, B. K. P., Schunck, B. G., Determining Optical Flow, *Artificial Intelligence*, *17* (1981), 1-3, pp. 185-203
[24] Lucas, B. D., Kanade, T., An Iterative Image Registration Technique with an Application to Stereo Vision, *Proceedings*, 7th International Joint Conference on Artificial Intelligence, San Francisco, Cal., USA 1981, pp. 674-679

Paper submitted: May 2, 2016
Paper revised: May 19, 2017
Paper accepted: May 20, 2017